Evaluation of conversion coefficients relating air-kerma to $H^*(10)$ using primary and transmitted x-ray spectra in the diagnostic radiology energy range

2016 J. Radiol. Prot. 36 117

(http://iopscience.iop.org/0952-4746/36/1/117)

IOP Publishing | Society for Radiological Protection Journal of Radiological Protection
J. Radiol. Prot. **36** (2016) 117–132 doi:10.1088/0952-4746/36/1/117

Evaluation of conversion coefficients relating air-kerma to *H**(10) using primary and transmitted x-ray spectra in the diagnostic radiology energy range

J C Santos[1], L Mariano[1], A Tomal[2] and P R Costa[1]

[1] Instituto de Física da Universidade de São Paulo, SP, Brazil
[2] Instituto de Física Gleb Wataghin, Universidade Estadual de Campinas, SP, Brazil

E-mail: josilene@usp.br and pcosta@if.usp.br

Received 24 February 2015, revised 3 November 2015
Accepted for publication 19 November 2015
Published 2 February 2016

Abstract

According to the International Commission on Radiation Units and Measurements (ICRU), the relationship between effective dose and incident air-kerma is complex and depends on the attenuation of x-rays in the body. Therefore, it is not practical to use this quantity for shielding design purposes. This correlation is adopted in practical situations by using conversion coefficients calculated using validated mathematical models by the ICRU. The ambient dose equivalent, *H**(10), is a quantity adopted by the IAEA for monitoring external exposure. Dose constraint levels are established in terms of *H**(10), while the radiation levels in radiometric surveys are calculated by means of the measurements of air-kerma with ion chambers. The resulting measurements are converted into ambient dose equivalents by conversion factors. In the present work, an experimental study of the relationship between the air-kerma and the operational quantity ambient dose equivalent was conducted using different experimental scenarios. This study was done by measuring the primary x-ray spectra and x-ray spectra transmitted through materials used in dedicated chest radiographic facilities, using a CdTe detector. The air-kerma to ambient dose equivalent conversion coefficients were calculated from these measured spectra. The resulting values of the quantity ambient dose equivalent using these conversion coefficients are more realistic than those available in the literature, because they consider the real energy distribution of primary and transmitted x-ray beams. The maximum difference between the obtained conversion coefficients and the constant value recommended in national and international radiation protection standards is 53.4%. The conclusion based on these results is that a constant coefficient may not be adequate for deriving the ambient dose equivalent.

Keywords: radiological protection, ambient dose equivalent, conversion coefficients

(Some figures may appear in colour only in the online journal)

1. Introduction

The quantities recommended for radiation protection purposes for external beams were defined by the International Commission on Radiological Protection (ICRP 2007) and by the International Commission on Radiation Units and Measurements (ICRU 1998). These quantities are classified as basic physical quantities, protection quantities and operational quantities, according to their properties and applications.

The basic physical quantities are the basis for the quantitative characterisation of external radiation beams, and their units are directly derived from primary quantities (Stadtmann 2001). However, the radiation dose limits are based on protection quantities that are not directly measurable. Therefore, the ICRP and ICRU proposed a set of operational quantities to provide a conservative estimation of the protection quantities, and recommended the use of these operational quantities for the routine monitoring of occupational exposure purposes (Stadtmann 2001).

Although the protection quantities cannot be directly measured, they may be calculated by using their correlation to basic physical quantities determined experimentally—or they can also be obtained by computer simulation (Turner 2007). This correlation is performed by conversion coefficients, which connect the basic physical quantities, such as air-kerma, absorbed dose or fluence, to the protection and operational quantities (ICRU 1998, ICRP 2010).

There is a limit to the available conversion coefficients for application in diagnostic radiology, since they are restricted to monoenergetic radiation beams. Reference conversion coefficients for monoenergetic photons recommended in the ICRU report 57 (ICRU 1998) show a strong energy dependence. Nevertheless, because of practical limitations, the national regulations usually adopt a constant factor for this conversion (Brazil 1998).

ICRU report 57 (ICRU 1998) recommends that mean or effective conversion coefficients must be used for equivalent dose ambient ($H^*(d)$) calculations from air-kerma measured in broad energy spectra. This can be determined by a weighted integration over the entire energy spectrum of radiation. Therefore, for radiation fields presenting broad energy spectra, conversion coefficients weighted by the x-ray spectrum must be obtained in order for them to be used adequately (Stadtmann 2001). In cases where calculation of the effective dose is necessary, the correlation between the operational quantity $H^*(10)$ and this protection quantity can be estimated by using the data provided in paragraphs 324 and 325 of ICRU 57. It is important, however, to emphasise the restrictions on using this protection quantity in estimating doses for monitoring purposes. According to ICRP 103, operational quantities are measurable and in routine monitoring, the values of these quantities are taken as sufficiently precise for assessment of the effective dose.

Radiation surveys are usually required in order to evaluate the radiation levels in areas of potential risk for members of the public or radiation workers. The ambient dose equivalent at a 10 mm depth of the ICRU sphere ($H^*(10)$) was adopted by the IAEA (IAEA 2011, IAEA 1996, IAEA 2014) as the quantity for monitoring external exposure. This quantity was also adopted in Brazil as the reference value for quantifying ambient radiation levels when using ionising radiation sources. In practical situations, the quantity $H^*(10)$ is obtained by applying

a conversion coefficient to the air-kerma measured data, since the calibration of the area survey metres in photon fields are performed in terms of this quantity.

Conversion coefficients relating air-kerma to ambient dose equivalents are presented in the literature for monoenergetic fields (Wagner *et al* 1985, ICRU 1992, ICRU 1998). They can also be calculated for narrow x-ray spectra obtained by mathematic models (Kharrati and Zarrad 2004), estimated by using a Monte Carlo simulation of the transmitted x-ray spectrum (Peixoto *et al* 1992) and for the x-ray incident beam in the ICRU sphere (Nogueira *et al* 1999). However, the conversion coefficients presented in the literature do not take into account the modifications in the incident x-ray spectra due to the typical beam attenuators present in practical situations. In these cases, the accuracy of the applied coefficients could be improved by including in their calculation the changes in the shape and amplitude of spectra transmitted by the typical attenuating materials found in diagnostic imaging rooms, such as shielding materials introduced for radiation protection purposes or the chest bucky used in thoracic examinations. In this work, the term transmitted x-ray spectra refers to the experimental spectra measured behind the barrier. It includes non-attenuated photons and photons scattered by sets of attenuators.

X-ray beams used for diagnostic imaging procedures are significantly modified when they are transmitted by attenuating structures, such as the patient body and the image receptor system (Santos and Costa 2013). According to ICRU recommendations (ICRU 1998), a more realistic representation of the quantity ambient dose equivalent should result by taking into account this modified spectrum in the calculations of conversion coefficients relating air-kerma to $H^*(10)$.

The present work shows the results from the computation of conversion coefficients relating air-kerma to $H^*(10)$ taking into account the photon energy distributions transmitted by the typical attenuators used in diagnostic radiology imaging procedures and structural shielding materials. Primary x-ray spectra and x-ray spectra transmitted by combinations of an anthropomorphic phantom, image receptor system and barite mortar plates were measured using a CdTe detector (Santos *et al* 2014). Conversion coefficients were calculated from these measured spectra, considering the transmitted photon beam distributions obtained by adopting simulated clinical situations. These coefficients are only applicable for situations where a barite mortar is used as shielding material. However, the presented results can provide information about how these coefficients can, in general, be dependent on the energy spectrum.

2. Methods and materials

2.1. Calculation of mean conversion coefficients

According to (Kharrati and Zarrad 2004) the mean conversion coefficients relating air-kerma to ambient dose equivalents calculated at 10 mm depth in the ICRU sphere for radiation energy spectra can be expressed by:

$$\overline{C}_k = \frac{H^*(10)}{K_{\text{air}}} \tag{1}$$

In equation (1), $\overline{C}_k$ is the mean conversion coefficient, in [Sv/Gy], over the range of energies of interest to the specific application, $H^*(10)$ is the ambient dose equivalent, and K_{air} represents the air-kerma.

The conversion coefficients for monoenergetic radiation, $C_k(E)$, are provided by the ICRU (1998), and they result from the application of an analytical function proposed by Wagner

et al (1985) to fit the experimental data of conversion coefficients for monoenergetic photons. The analytical function proposed by Wagner *et al* (1985) was:

$$C_k(E) = \frac{z(E)}{a[z(E)]^2 + bz(E) + c} + d \times \arctan\{g.\,[z(E)]\ \} \tag{2}$$

In equation (2), $z(E) = \ln(E/E')$, E is the photon energy in keV, and E', a, b, c, d, and g are the fitting parameters of the function which were obtained by applying regression methods and statistical weights from experimental input data. By applying these methods, the authors (Wagner *et al* 1985) found the following results: $E' = 9.85\,\text{keV}$, $a = 1.465$, $b = -4.414$, $c = 4.789$, $d = 0.7006$, and $g = 0.6519$. The results of equation (2) represent conversion coefficients with strong energy dependence in the diagnostic energy range.

A computational method for the calculation of mean conversion coefficients for a broad spectra (non-monoenergetic) radiation beam was presented by Kharrati and Zarrad (2004). According to this method, mean conversion coefficients can be calculated by the integration of the conversion coefficients for monoenergetic radiation, $C_k(E)$, over the x-ray spectra as follows:

$$\overline{C}_k = \frac{\displaystyle\int_0^{E_{\max}} C_k(E)\phi(E)E\left(\frac{\mu_{\text{en}}(E)}{\rho}\right)_{\text{air}} \exp(-\mu(E)x)\mathrm{d}E}{\displaystyle\int_0^{E_{\max}} \phi(E)E\left(\frac{\mu_{\text{en}}(E)}{\rho}\right)_{\text{air}} \exp(-\mu(E)x)\mathrm{d}E} \tag{3}$$

In equation (3), $\phi(E)$ is the photon fluence as a function of energy, $(\mu_{\text{en}}(E)/\rho)_{\text{air}}$ is the mass-energy absorption coefficient for the air, $\exp(-\mu(E)x)$ represents the attenuation due to the thickness, x, of an attenuating material with the linear attenuation coefficient $\mu(E)$, and $E_{\max}$ is the maximum energy of the spectrum. In their calculations, Kharrati and Zarrad (2004) used the values of $\phi(E)$ obtained by a polynomial model (Boone and Seibert 1997).

The air-kerma x-ray spectrum, $N(E,x)$, transmitted by the thickness, x, of a given material can be represented by the following equation:

$$N(E,x) = \phi(E)E\left(\frac{\mu_{\text{en}(E)}}{\rho}\right)_{\text{air}} \exp(-\mu(E)x) \tag{4}$$

Using equation (4) and considering data from the primary and transmitted experimental spectra, equation (3) for the mean conversion coefficients can be rewritten as:

$$\overline{C}_k = \frac{\displaystyle\int_0^{E_{\max}} C_k(E)N(E,x)E\mathrm{d}E}{\displaystyle\int_0^{E_{\max}} N(E,x)\mathrm{d}E} \tag{5}$$

The air-kerma x-ray spectra, $N(E,x)$, can be characterised in terms of their first half value layer (HVL), which is a function of the maximum energy (in eV) of the spectra, $E_{\max}$, numerically equal to the applied voltage (in volts). The HVL is also related to the beam hardening of the spectra, represented by the thickness, x, of a reference material (usually aluminium). This quantity is experimentally determined by well-established methods (IAEA 2007).

Table 1. Standard radiation qualities RQR according to TRS 457 (IAEA 2007) and added filtration used (mm Al).

Radiation quality	x-ray tube voltage (kV)	First HVL (mm Al)	Added filtration (mm Al)[a]
RQR 3	50	1.78	2.94(1)
RQR 5	70	2.58	3.04(1)
RQR 8	100	3.97	3.74(1)
RQR 10	150	6.57	4.71(1)

[a] Burguer and Costa (2012).

Moreover, the air-kerma x-ray spectra can also be represented by their mean energy as follows:

$$E_{\mathrm{m}} = \frac{\int_0^{E_{\max}} EN(E,x)\mathrm{d}E}{\int_0^{E_{\max}} N(E,x)\mathrm{d}E} \tag{6}$$

Therefore, a dependence of the mean conversion coefficients calculated according to equation (5) can be identified with the first half-value layer and mean energy of the corresponding spectra. These dependences were considered in the representation of the results obtained in the present work.

2.2. Primary and transmitted spectra measurements

Diagnostic x-ray standard radiation qualities were established by the International Electrotechnical Commission in its publication IEC 61267 (IEC 2005). These x-ray beam qualities were adopted by the IAEA in the report TRS 457 (IAEA 2007) and are widely used in primary and secondary standard dosimetry laboratories (PSDL and SSDL, respectively). Table 1 shows the characteristics of the RQR standard radiation qualities and the added aluminium filtration used in the present study for obtaining the beam qualities according to TRS 457.

Primary and transmitted spectra were measured in the present work to be used for calculating the mean conversion coefficients as presented in equation (5). The primary spectra were measured in all available radiation qualities, from RQR 2 to RQR 10. The transmitted spectra were measured using the beam qualities RQR 3, 5, 8 and 10 presented in table 1. The transmitted spectra were configured using the sets of attenuators listed below and shown in figure 1.

- Barite mortar plates with nominal thicknesses of 5, 10, 15, 20, 25 mm. These plates were positioned in the central axis of the radiation beam (figure 1(a)).
- Barite mortar plates in combination with a computer radiology image plate (Agfa, Inc., Belgium) and an 8:1 anti-scatter grid (Kiran Medical Systems, India) with dimensions of 30 cm × 40 cm and 40 lines cm^{-1} (figure 1(b)).
- Barite mortar plates in combination with an image plate, anti-scatter grid and a 5 year-old anthropomorphic phantom (Cirs, Inc., USA) for simulating a paediatric patient (figure 1(c)).
- Barite mortar plates in combination with an image plate, anti-scatter grid and a standard adult anthropomorphic RANDO phantom (Alderson Research Laboratories, USA) for simulating an adult patient (figure 1(d)).

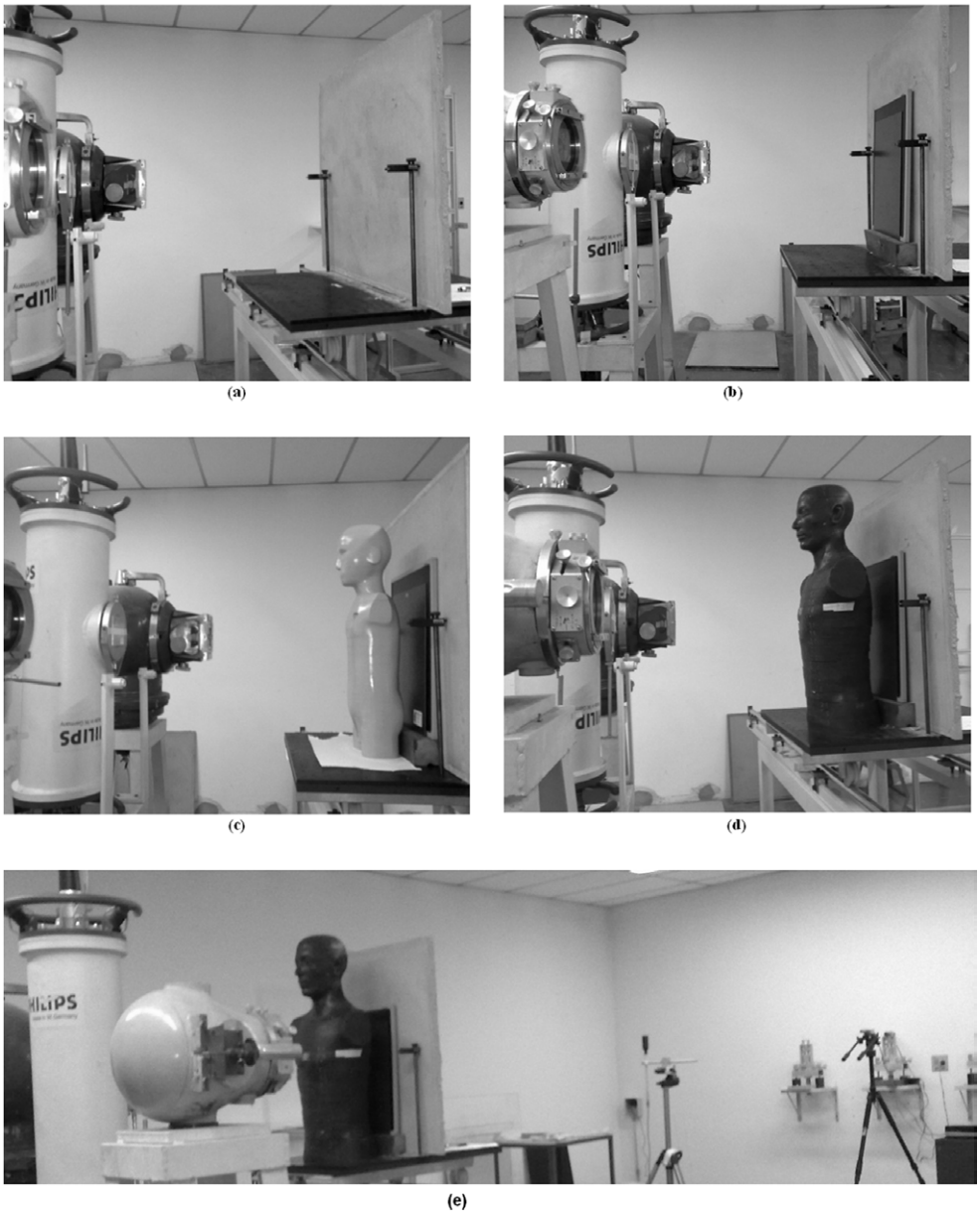

Figure 1. Experimental setup: (a) for the transmitted spectra measurements through barite mortar plates of different thicknesses; (b) for transmitted spectra measurements through mortar plates in combination with an image plate and an anti-scatter grid; (c) for transmitted spectra measurements through mortar plates in combination with an image plate, an anti-scatter grid and a paediatric patient simulator; (d) for transmitted spectra measurements through mortar plates in combination with an image plate, an anti-scatter grid and an adult patient simulator; (e) positioning of the attenuators, ionisation chamber and spectrometer.

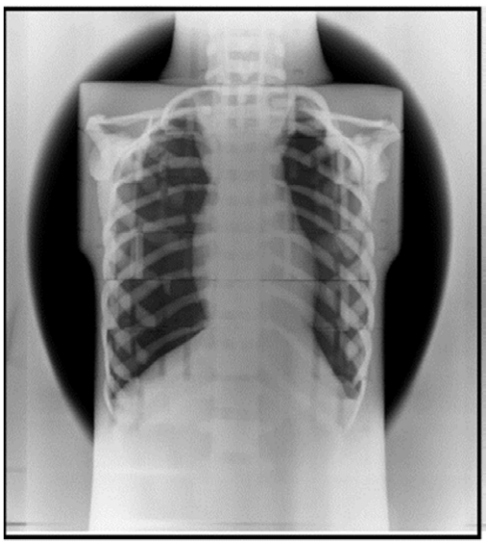

Figure 2. Radiographic image of the paediatric anthropomorphic phantom in an x-ray field.

Both primary and transmitted x-ray spectra were measured using a $3 \times 3\,mm^2$ CdTe spectrometer model XR-100T (Amptek, Inc., Bedford, MA, USA). This detector was coupled to a tungsten collimator 1 mm in diameter in order to limit the photon fluence, reducing pile-up effects and ensuring the reduction of carrier collection in the borders of the detector (Fink *et al* 2006). Additionally, air-kerma were measured simultaneously to the spectra by using an ionisation chamber model TW23361 (PTW Inc., Freiburg, Germany). This chamber was calibrated against a traceable standard in a secondary standard dosimetry laboratory (SSDL).

The x-ray beam size was selected according to the area of the chest region in anthropomorphic phantoms. Both paediatric and adult anthropomorphic phantoms were positioned at 1 m from the x-ray tube focal spot. These selections defined a 13.10(4) cm field diameter in the chest region of the paediatric phantom and 21.56(4) cm field diameter in the chest region of the adult phantom. Figure 2 shows a radiographic image of the paediatric phantom using the described beam arrangement.

Figure 3 presents the experimental set-up adopted for the spectra measurements and shows the positioning of the measuring devices. The primary beam x-ray spectra were determined with the photons impinging directly on the detector. Transmitted x-ray spectra were measured with the attenuating materials (phantoms, barite mortars, anti-scatter grids and image plate), combined as described previously (figure 1). These materials were positioned between the x-ray tube and the ionisation chamber, intercepting the primary beam; they are not shown in figure 3.

A computer routine written in Matlab version 7.8 (*The MathWorks Inc*., USA) was developed to correct the measured spectra by the response function of the CdTe detector for radiological x-ray energies (Santos and Costa 2013). The stripping procedure described by Di Castro *et al* (1984) and presented in equation (7) was applied in these corrections. This procedure takes into account K-escape, Compton scattering and detector efficiency corrections.

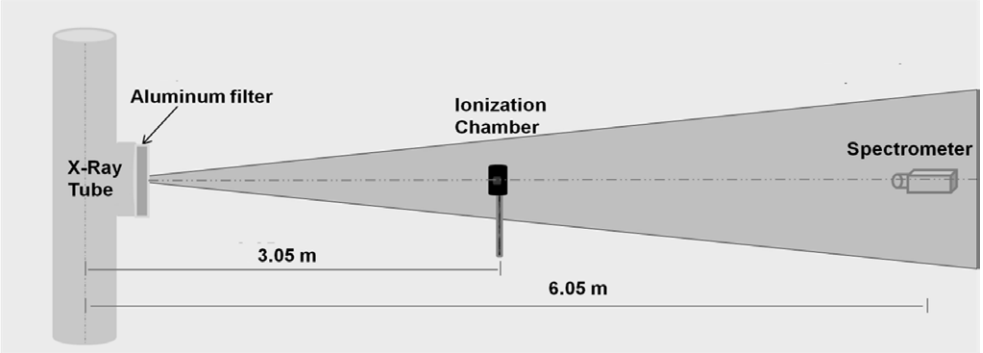

Figure 3. Scheme for primary and transmitted x-ray spectra measurements. Air-kerma measurements were performed for each x-ray irradiation. Primary x-ray spectra were measured with the beam impinging on the detector. Transmitted x-ray spectra were measured with a combination of attenuating materials positioned between the x-ray tube and the ionisation chamber intercepting the beam.

$$N_t(E_0) = \frac{\left(N_d(E_0) - \eta_k(E_0 + E_k) N_t(E_0 + E_k) - \sum_{E=E_c(E_0)}^{E_{max}} f N_t(E) \right)}{\varepsilon(E_0)} \tag{7}$$

In equation (7), $N_t(E_0)$ is a true number of photons with energy E_0, $N_d(E_0)$ is a detected number of photons with energy E_0, $\eta_k(E_0 + E_k)$ is the fraction of K-escape photons of energy $(E_0 + E_k)$, $N_t(E_0 + E_k)$ is the true number of photons of energy $(E_0 + E_k)$, $E_c(E_0)$ is the energy of a photon that has Compton edge energy E_0, $f = \eta_c/C$ is the ratio between Compton efficiency and the channel number, and $\varepsilon(E_0)$, is the full energy peak efficiency.

The correction method for distortion due to Compton scattering and the determination of Compton efficiency is described by Terini *et al* (1999). The detector efficiency and fluorescent escape fraction were obtained by Monte Carlo simulation using the PENELOPE code (Salvat 2003). These quantities were originally calculated for mammographic x-ray energies (5–40 keV) (Tomal *et al* 2012) and recently extended for diagnostic energies (40–150 keV) (Tomal *et al* 2014).

The implemented algorithm corrects the raw spectra by the response function of the CdTe detector and normalises the area under the spectrum by the corresponding air-kerma value that is measured simultaneously using the ionisation chamber. It also performs the energy calibration of the spectrum using experimental data obtained by standard gamma emitter radiation sources (^{241}Am, ^{133}Ba, ^{152}Eu). Therefore, the output of the developed computer programme represents the corrected spectrum in units of [mGy/mAs.keV@1m]. Comparisons of the measured primary spectra corrected by this programme showed good agreement with the spectra generated by the TBC semi-empirical model (Costa *et al* 2007).

2.3. Determination of beam qualities and conversion coefficients

The HVL was measured for primaries and transmitted spectra by adding aluminium filters of different thicknesses between the x-ray tube windows (for the primary spectra) and after the transmission setup (for the transmitted spectra). It was not possible to measure HVL for low-intensity transmitted x-ray beams due to instrumental limitations. Additionally, the mean

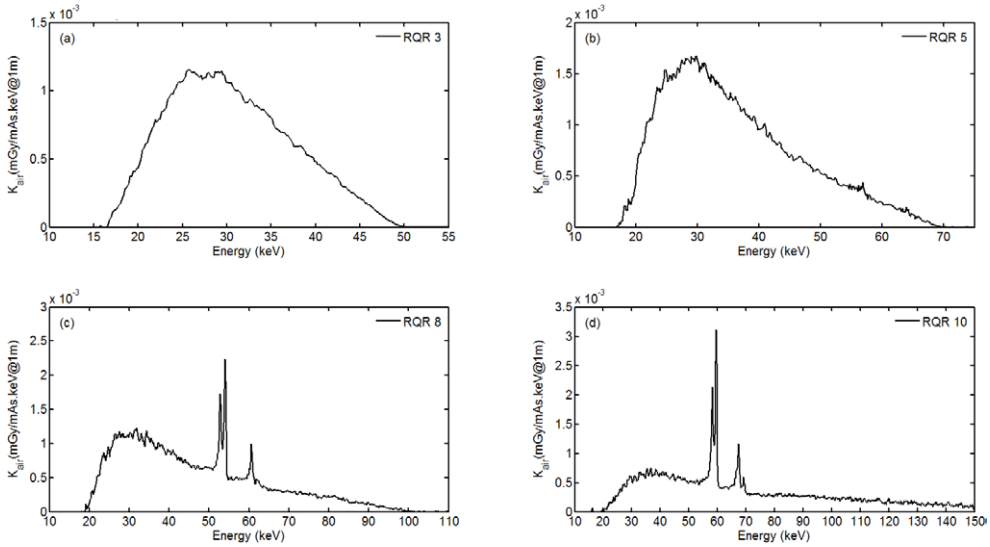

Figure 4. Corrected x-ray spectra corresponding to the radiation qualities (a) RQR3, (b) RQR 5, (c) RQR 8 and (d) RQR 10. Table 1 presents the voltage and filtration combinations for each configuration.

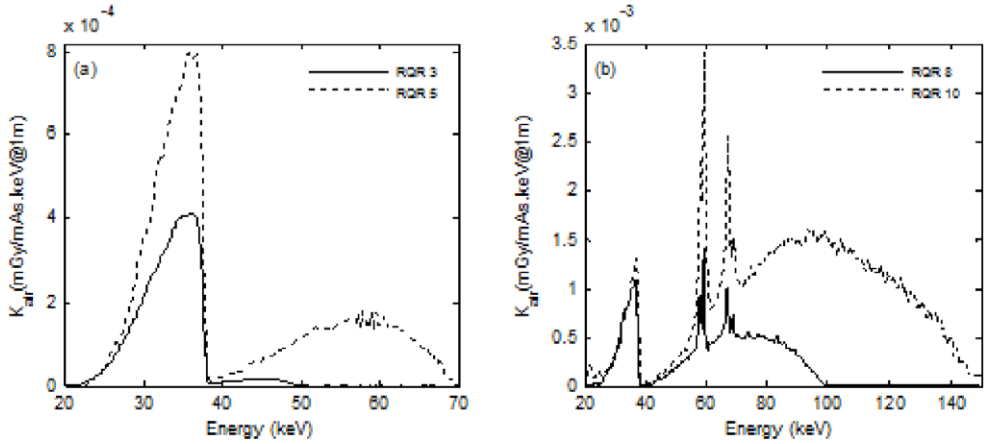

Figure 5. Transmitted spectra through a barite mortar plate of 5 mm nominal thickness for incident beam qualities (a) RQR 3 and RQR 5 and (b) RQR8 and RQR10.

energy of each spectrum was calculated using equation (6). Finally, each measured spectrum was used as input to equation (5) for the evaluation of the mean conversion coefficient for each measuring condition. The number of counts at the measured spectra was controlled in order to assure an uncertainty of lower than 5%.

3. Results

Primary x-ray beams for all qualities presented in table 1 were measured. As an example, figure 4 shows the corrected primary spectra for the beam qualities RQR 3, 5, 8 and 10. These qualities were used as incident beams for all the transmitted spectra measured in this study.

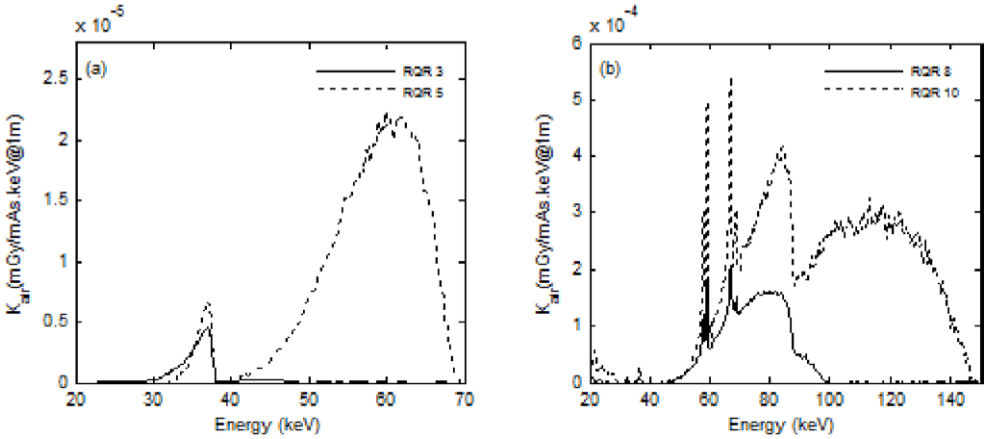

Figure 6. Transmitted spectra through a barite mortar plate of 5 mm nominal thickness, image plate and anti-scatter grid for incident beam qualities (a) RQR 3 and RQR 5 and (b) RQR8 and RQR10.

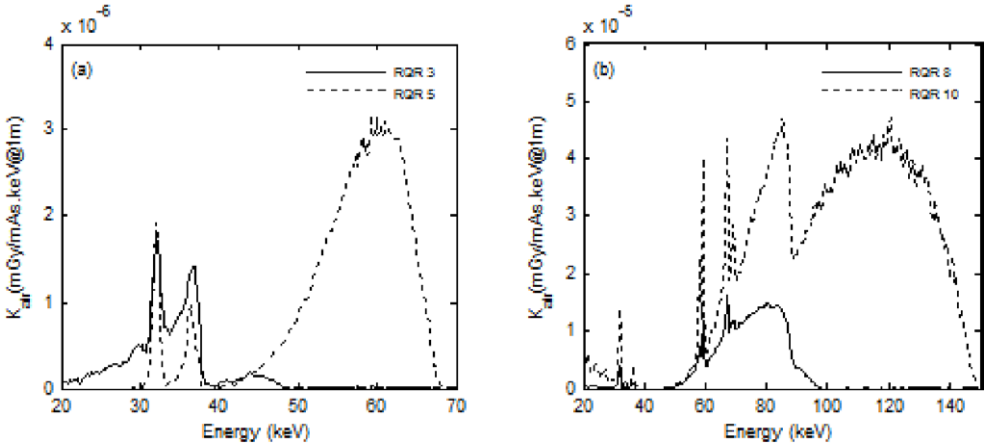

Figure 7. Transmitted spectra through a barite mortar plate of 5 mm nominal thickness, image plate, anti-scatter grid and paediatric patient simulator for incident beam qualities (a) RQR 3 and RQR 5 and (b) RQR8 and RQR10.

Figure 5 shows the spectra transmitted through a barite mortar plate with 5 mm nominal thickness. Figure 6 shows the spectra transmitted through a barite mortar plate of 5 mm nominal thickness in combination with the computed radiology image plate and an anti-scatter grid. Figure 7 shows the spectra transmitted through a barite mortar plate of 5 mm nominal thickness in combination with the computed radiology image plate, anti-scatter grid and the paediatric phantom. Finally, figure 8 shows the spectra transmitted through a barite mortar plate of 5 mm nominal thickness in combination with the computed radiology image plate, anti-scatter grid and the adult phantom. The figures show the results of the transmitted spectra considering each beam quality adopted in the present work. All measured spectra were corrected and normalised in order to be presented in terms of air-kerma distributions per mAs per keV at 1 m distance from the x-ray tube focal spot.

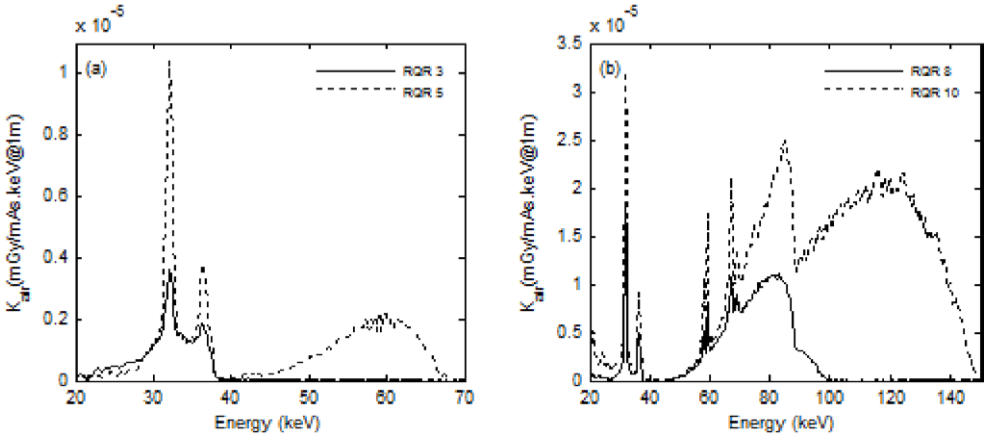

Figure 8. Transmitted spectra through a barite mortar plate of 5 mm nominal thickness, image plate, anti-scatter grid and adult patient simulator for incident beam qualities (a) RQR 3 and RQR 5 and (b) RQR8 and RQR10.

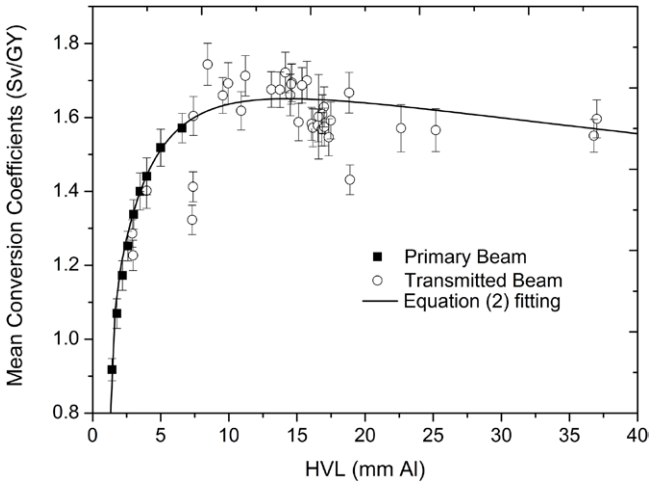

Figure 9. Mean conversion coefficients (Sv/Gy) relating air-kerma to $H^*(10)$ as a function of the HVL for x-ray primary beams (filled points) and transmitted x-ray beams through the set of attenuators presented in figure 1 (unfilled points). The line represents a fitting of equation (2).

These transmitted spectra (figures 5–8) are significantly reduced in intensity when attenuators are added to the experimental setup. Moreover, they present intense absorption in energy proximally 39 keV related to the K-edge absorption of the barium present in barite mortar plate. The peaks in energies 32.19 keV and 36.37 keV, present in some of the spectra are the barium fluorescence lines. The narrow lines at energies of 59.3 keV and 67.2 keV are related to the characteristic x-ray emissions of the tungsten target. The measured spectra transmitted by a combination of attenuators that include the anti-scatter grid for RQR 8 and RQR 10 incident beam qualities presented an absorption edge at 88.0 keV. This energy corresponds to the K-edge absorption of the lead present in this anti-scatter grid.

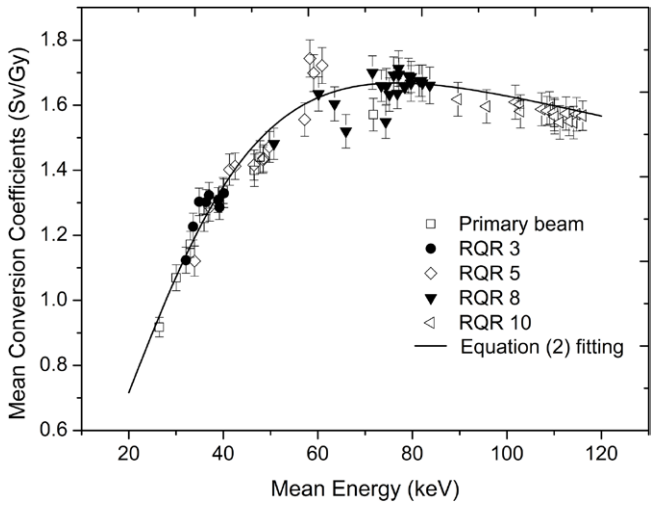

Figure 10. Mean conversion coefficients relating air-kerma to $H^*(10)$ as a function of the mean energy, for x-ray primary beams and x-ray beam qualities RQR 3, RQR 5, RQR 8 and RQR 10 transmitted through the set of attenuators presented in figure 1. The line represents a fitting of equation (2).

From each measured spectra, the mean conversion coefficient for each measuring condition was computed, as described in equation (5). These mean coefficients were related to the measured HVLs and to the calculated mean energies (equation (6)).

Figures 9 and 10 show the mean conversion coefficients relating air-kerma to $H^*(10)$ as a function of the half value layer (HVL) and mean energy, respectively. The uncertainties of these coefficients were estimated based on the experimental air-kerma uncertainties obtained from the ionization chamber data. The maximum calculated uncertainty was 3.7%.

The solid line in each figure represents the fitting of the function presented in equation (2). The least-square method was used in order to determine the best fitting parameters for each set of experimental data. The fitting parameters for equation (2) and the corresponding R^2 are presented in table 2.

Table 3 presents some of the conversion coefficient values obtained from the transmitted spectra through different sets of attenuators with the respective values of the HVL. The HVL was estimated from the x-ray measured spectrum. Conversion coefficient values vary from 1.18 to 1.74 and did not vary linearly with the HVL.

As an example of how to apply the obtained result, a dedicated chest room with a 20 mm barite mortar wall could be considered. Considering that the distance of the focal spot to this primary barrier is 3.5 m and that a CR image receptor and an anti-scatter grid are used in all the procedures, this is very realistic. An x-ray tube filtration equivalent to the standard quality RQR8 should also be taken into account. An additional consideration is that the procedures are conducted using 100 kV, and that the workload is 0.6 mA min/week per patient and finally that the images of 120 patients are taken per week (NCRP 2004). The area survey using a calibrated ion chamber measured an air-kerma rate of 7.9 mGy/week. If compliance with the local standards needs to be reported in ambient dose equivalent, the radiation protection

Table 2. Parameters for fitting equation (2) to the resulting mean conversion coefficients relating air-kerma to $H^*(10)$ presented in figures 9 and 10 as a function of HVL and mean energy, respectively.

	The fit parameters referring to figure 9	The fit parameters referring to figure 10
Parameters	Value	Value
E_o	1[a]	9.85[a]
a	0.004(1)	0.006(5)
b	0.07(4)	0.001(5)
c	0.08(2)	0.09(5)
d	−6(3)	−17(9)
g	1.2(5)	0.6[a]
	$R^2 = 0.86$	$R^2 = 0.96$

[a] Values fixed during the fitting process.
Note: The numbers in brackets represent uncertainties in the last decimal place.

Table 3. Conversion coefficient from air-kerma to ambient dose equivalent obtained from transmitted spectra through different sets of attenuators with respective values of HVL.

	Transmitted spectrum HVL (mmAL)	Conversion coefficients (Sv/Gy)	Transmitted spectrum HVL (mmAL)	Conversion coefficients (Sv/Gy)
Incident spectrum (kV)	Attenuation set: 5 mm barite mortar plate		Attenuation set: anti-scatter grid + image plate + 5 mm barite mortar plate	
50 (RQR 3)	2.9	1.22	3.5	1.3
70 (RQR 5)	4.1	1.40	8.9	1.74
100 (RQR 8)	7.9	1.60	11.5	1.71
150 (RQR 10)	12.1	1.62	13.8	1.62
Incident spectrum (kV)	Attenuation set: paediatric chest phantom + anti-scatter grid + image plate + 5 mm barite mortar plate		Attenuation set: adult chest phantom + anti-scatter grid + image plate + 5 mm barite mortar plate	
50 (RQR 3)	3.3	1.26	2.7	1.18
70 (RQR 5)	8.2	1.70	4.8	1.47
100 (RQR 8)	11.4	1.70	10.1	1.65
150 (RQR 10)	14.2	1.60	13.4	1.60

officer must convert this air-kerma rate value to the standardised quantity. Some countries adopt the constant value of 1.14 Sv/Gy as a conversion coefficient for these quantities. By applying this conversion coefficient, the ambient dose equivalent results in 9.0×10^{-3} mSv/week. However, the conversion coefficient for this practical situation (chest examination with 20 mm of barite mortar, patient into the beam, anti-scatter grid and image receptor) obtained in the present work is 1.55 Sv/Gy, resulting in 1.2×10^{-2} mSv/week. This value is 33% higher than that obtained by using the standard conversion coefficient defined by local regulation. Additionally, if the radiation protection goal for this area is considered to be 0.01 mSv/week

(uncontrolled areas), the example results present contradictory conclusions in terms of shielding adequacy for this area.

4. Conclusion

Mean conversion coefficients relating air-kerma to $H^*(10)$ were calculated using experimental measured spectra considering the attenuation provided for materials usually present in radiological image procedures. The measured spectra indicated that significant changes in incident energy distribution occur for each specific set of attenuators. The mean conversion coefficients were obtained for a large set of beam qualities in this work, and they were presented as a function of both the HVL and mean energy. The results presented in figures 9 and 10 highlight the energy dependence of these conversion coefficients. This means that the most adequate method for converting air-kerma to $H^*(10)$ should consider the energy spectra. This indicates that the mean conversion coefficient should be calculated for each specific spectrum distribution. This result strengthens the recommendation of ICRU 57 for calculating these coefficients for broad energy spectra—similar to the x-ray beams used in imaging procedures.

Additionally, conversion coefficients should be adequately calculated to avoid systematic errors in the estimation of the ambient dose equivalent. For example, in spite of the strong energy dependence of these coefficients for monoenergetic photons in the diagnostic energy range, local regulations adopt a constant coefficient equal to 1.14 Sv/Gy for converting air-kerma to ambient dose equivalent. The results achieved by methods applied in the present study are greater than this constant coefficient up to 53.4%. Therefore, $H^*(10)$ obtained by the constant coefficient 1.14 Sv/Gy may not be adequate for representing environmental doses to evaluate the adequacy of the shielding barrier. The main consequence of this fact is that the thickness of primary shielding barriers may be underestimated and the protection of workers and members of public may not comply with international requirements.

Finally, it is important to add that ICRU 57 (paragraph 325) presents a maximum overestimation of 15% of the effective dose when compared to equivalent ambient dose using conversion factor ratios only. The correlation between the operational quantity $H^*(10)$ and this protection quantity, E, can be estimated by using data provided in paragraphs 324 and 325 of the ICRU 57.

Acknowledgments

The authors thank the FAPESP for financial support under project number 2011/04721-9 and research regular project 2010/12237-7, the CNPq for support through project 312029/2009-8 and the CNPq/FAPESP for funding of the project by INCT—Metrology of ionising radiation in medicine.

Appendix A. Conversion coefficients

Table A1 presents the conversion coefficients obtained for each incident beam used in this study considering all sets of attenuators used.

Table A1. Conversion coefficient from air-kerma to ambient dose equivalent obtained from transmitted spectra through different sets of attenuators.

	Conversion coefficients (Sv/Gy)			
	Incident beams			
Sets of attenuators	RQR 3	RQR 5	RQR 8	RQR 10
B5	1.23	1.409	1.60	1.62
B5 + SET1	1.32	1.749	1.71	1.63
B5 + SET2	1.26	1.70	1.70	1.61
B5 + SET3	1.18	1.47	1.66	1.60
B10	1.29	1.44	1.66	1.60
B10 + SET1	1.33	1.72	1.69	1.59
B10 + SET2	1.37	1.73	1.69	1.59
B10 + SET3	1.17	1.34	1.63	1.58
B15	1.30	1.41	1.68	1.58
B15 + SET1	1.36	1.68	1.69	1.57
B15 + SET2	1.27	1.35	1.67	1.57
B15 + SET3	1.24	1.33	1.63	1.57
B20	1.31	1.43	1.67	1.58
B20 + SET1	1.40	1.63	1.69	1.57
B20 + SET2	1.24	1.27	1.66	1.57
B20 + SET3	1.10	1.19	1.55	1.57
B25	1.30	1.42	1.66	1.57
B25 + SET1	1.250	1.56	1.67	1.55
B25 + SET2	1.10	1.17	1.64	1.55
B25 + SET3	1.00	1.12	1.52	1.55

Note: The sets of attenuators are composed of barite mortar plates with different thicknesses, e.g. B5 and B20 represent 5 mm and 20 mm barite mortar plates respectively. SET1 represents the attenuation set: anti-scatter grid + image plate; SET2 represents the attenuation set: paediatric chest phantom + anti-scatter grid + image plate and finally, SET3 represents the attenuation set: adult chest phantom + anti-scatter grid + image plate. These conversion coefficients present 3.7% maximum uncertainty.

References

Boone J M and Seibert J A 1997 An accurate method for computer-generating tungsten anode x-ray spectra from 30 to 140 kV *Med. Phys.* **24** 1661–70

Brasil 1998 Portaria n°453, de 1°de junho de 1998 *Agência Nacional De Vigilância Sanitária* (www.conter.gov.br/uploads/legislativo/portaria_453.pdf)

Burguer A A and Costa P R 2012 Implementação e Validação de Qualidades de Feixes de Raios X Segundo o Código de Prática da IAEA *Simposio Int. Sobre Protección Radiológica* (Cuzco: SPR)

Costa P R, Nersissian D Y, Salvador F C, Rio P B and Caldas L V E 2007 Generation of calibrated tungsten target x-ray spectra: modified TBC model *Health Phys.* **92** 24–32

Di Castro E, Pani R, Pellegrini R and Bacci C 1984 The use of cadmium telluride detectors for the qualitative analysis of diagnostic x-ray spectra *Phys. Med. Biol.* **29** 1117–31

Fink J, Krüger H, Lodomez P and Wermes N 2006 Characterization of charge collection in CdTe and CZT using the transient current technique *Nucl. Instrum. Methods Phys. Res.* A **560** 435–43

IAEA 1996 *International Basic Safety Standards for Protection Against Ionizing Radiation and for the Safety of Radiation Sources* (*Safety Series* vol 115) (Vienna: International Atomic Energy Agency)

IAEA 2007 *Dosimetry in Diagnostic Radiology: an international Code of Practice* (Vienna: International Atomic Energy Agency)

IAEA 2011 *Implementation of the International Code of Practice on Dosimetry in Diagnostic Radiology (TRS 457): Review of Test Results* (Vienna: International Atomic Energy Agency)
IAEA 2014 Radiation protection and safety of radiation source: international basic safety standards *IAEA Safety Standards Series* (Vienna: International Atomic Energy Agency)
ICRP 2007 Recommendations of the Int. Commission on Radiological Protection. ICRP Publication 103 *Ann. ICRP* **37** (2–4)
ICRP 2010 Conversion coefficients for radiological protection quantities for external radiation exposures. ICRP publication 116 *Ann. ICRP* **40** (2–5)
ICRU 1998 Conversion coefficients for use in radiological protection against external radiation *ICRU Report No. 57* (Bethesda, MD: ICRU)
ICRU 1992 Measurement of dose equivalents from external photon and electron radiations *ICRU Report No. 47* (Bethesda, MD: ICRU)
IEC 2005 *Medical Diagnostic X-ray Equipment—Radiation Conditions for Use in the Determination of Characteristics. IEC 61267* (Geneva: International Electrotechnical Commission)
Kharrati H and Zarrad B 2004 Computation of conversion coefficients relating air kerma to Hp(0.07,α), Hp(10,α), and $H^*(10)$ for x-ray narrow spectrum from 40 to 140 kV *Med. Phys.* **31** 277–84
NCRP 2004 Structual shielding design for medical x-ray imaging facilities *NCRP Report No. 147* (Bethesda MD: NCRP)
Nogueira M S, Campos L L and Mota H C 1999 Determination of conversion coefficients between air kerma or photon fluence and ambient dose equivalent for diagnostic x-ray beams *Radiat. Protect. Dosim.* **81** 123–32
Peixoto J E, Drexler G and Zankl M 1992 Attenuation factors for x-rays in terms of ambient and effective dose equivalent *Radiat. Protect. Dosim.* **43** 119–21
Salvat F *et al* 2003 *PENELOPE: a Code System for Monte Carlo Simulation of Electron and Photon Transport* (Illy-les-Moulineaux: Nuclear Energy Agency)
Santos J C and Costa P R 2013 Evaluation of the effective energy of primary and transmitted workload weighted x-ray spectra *Radiat. Phys. Chem.* **95** 221–3
Santos J C, Tomal A, Mariano L and Costa P R 2014 Application of a semi-empirical model for the evaluation of transmission properties of barite mortar *Appl. Radiat. Isot.* **100** 38–42
Stadtmann H 2001 Dose quantities in radiation protection and dosimeter calibration *Radiat. Protect. Dosim.* **96** 21–6
Terini R A, Costa P R, Furquim T A C and Herdade S B 1999 Measurements of discrete and continuous x-ray spectra with a photodiode at room temperature *Appl. Radiat. Isot.* **50** 343–54
Tomal A, Cunha D M, Antoniassi M and Poletti M E 2012 Response functions of Si(Li), SDD and CdTe detectors for mammographic x-ray spectroscopy *Appl. Radiat. Isot.* **70** 1355–9
Tomal A, Santos J C, Costa P R, Lopez Gonzales A H and Poletti M E 2014 Monte Carlo simulation of the response functions of CdTe detectors to be applied in x-ray spectroscopy *Appl. Radiat. Isot.* **100** 32–7
Turner J E 2007 *Atoms, Radiation, and Radiation Protection* (Weinheim: Wiley)
Wagner S R, Grosswendt B, Harvey J R, Mill A J, Selbach H J and Siebert R L 1985 Unified conversion functions for the new ICRU operational radiation protection quantities *Radiat. Protect. Dosim.* **12** 231–5